

# Tunneling spectra of layered strongly correlated $d$ -wave superconductors

Tiago C. Ribeiro<sup>1,2</sup> and Xiao-Gang Wen<sup>3</sup>

<sup>1</sup>*Department of Physics, University of California, Berkeley, California 94720, USA*

<sup>2</sup>*Material Sciences Division, Lawrence Berkeley National Laboratory, Berkeley, California 94720, USA*

<sup>3</sup>*Department of Physics, Massachusetts Institute of Technology, Cambridge, Massachusetts 02139, USA*

(Dated: December 5, 2018)

Tunneling conductance experiments on cuprate superconductors exhibit a large diversity of spectra that appear in different nano-sized regions of inhomogeneous samples. In this letter, we use a mean-field approach to the  $tt't''J$  model in order to address the features in these spectra that deviate from the BCS paradigm, namely, the bias sign asymmetry at high bias, the generic lack of evidence for the Van Hove singularity, and the absence of coherence peaks at low dopings. We conclude that these features can be reproduced in homogeneous layered  $d$ -wave superconductors solely due to a proximate Mott insulating transition. We also establish the connection between the above tunneling spectral features and the strong renormalization of the electron dispersion around  $(0, \pi)$  and  $(\pi, 0)$  and the momentum space anisotropy of electronic states observed in ARPES experiments.

*Introduction* – Tunneling and angle-resolved photoemission spectroscopy (ARPES) are unique experimental techniques in that they probe the single electron microscopic physics of strongly correlated systems like the cuprate  $d$ -wave superconductors (dSC). Even though both techniques support the presence of well defined Bogoliubov nodal quasiparticles in these materials, away from the nodes deviations from the BCS paradigm are encountered [1, 2, 3, 4, 5, 6, 7, 8, 9]. Simultaneously describing these deviations in ARPES and tunneling experiments is of utmost importance to understand the nature of the underlying strong local correlations.

In this letter, we focus on the differential conductance measured by scanning tunneling microscopy (STM) experiments on the cuprates. In particular, we address three key aspects observed in the data as the electron concentration is increased toward half-filling, namely, *(i)* an increasing asymmetry of spectra for large positive and negative bias; *(ii)* the ubiquitous absence of peaks caused by the underlying Van Hove (VH) singularities in the quasiparticle density of states (DOS); *(iii)* the gradual depletion of the superconducting (SC) coherence peaks.

First, we argue that BCS expectations for dSC are at odds with the above features. BCS theory generally predicts that tunneling spectra of quasi-2D SC materials display VH singularity peaks in addition to two SC coherence peaks [10, 11]. However, these VH peaks are not observed by experiments in different cuprate families (Bi2212 [3, 5, 12, 13, 14], Bi2201 [15], LSCO [14], YBCO [16]). Notably, even the SC coherence peaks are absent in certain tunneling spectra [3, 4, 5, 6, 17].

We then show that the aforementioned non-trivial spectral features are reproduced in homogeneous SC systems close to the Mott insulating state. Specifically, we use a mean-field (MF) theory of doped Mott insulators [18, 19] that accounts for many fingerprints of strong correlation physics in ARPES data, including the strong band renormalization close to  $(0, \pi)$  and  $(\pi, 0)$  [20] and the sharp momentum space anisotropy of electronic

states, known as the nodal-antinodal dichotomy [7, 8, 9], which we show are intimately connected to STM data. We thus obtain a consistent theoretical microscopic description of ARPES and tunneling spectroscopy. Moreover, we explicitly show that the above deviations from BCS spectra follow from how the local electron Coulomb repulsion and the resulting short-range antiferromagnetic (AF) correlations affect the phenomenology of dSC.

*Tunneling spectra of BCS  $d$ -wave superconductors* – We consider the tunneling across a normal-metal – insulator – superconductor junction in the case of a 2D superconductor. Assuming specular transmission across a thin planar junction within the elastic channel, the differential tunneling conductance perpendicular to the 2D layers can be essentially equated to the quasiparticle DOS [21, 22] and, at zero temperature, it is given by [23]

$$\frac{dI}{dV} = 4e\pi M^2 N(E_F) \sum_{\mathbf{k}} A(V, \mathbf{k}) \quad (1)$$

where  $M$  is the tunneling matrix element,  $N(E_F)$  is the normal-metal DOS,  $V$  is the bias of the SC sample with respect to the metal and  $A(\omega, \mathbf{k})$  is the electron spectral function in the SC sample. The sum in (1) is over the 2D layer's Brillouin zone.

In Fig. 1 we use (1) together with the well known results for the BCS electron spectral function [23] to plot the BCS tunneling differential conductance. In particular, we take the normal state dispersion  $\varepsilon_{\mathbf{k}}$  determined by the  $1^{st}$ ,  $2^{nd}$  and  $3^{rd}$  nearest-neighbor (NN) hopping parameters  $t$ ,  $t'$  and  $t''$  with  $t' = -2t'' = -0.12t$  [24] so that the normal state Fermi surface lies close to  $(0, \pi)$  when the electron density is  $1 - x = 0.80$  (inset of Fig. 1), as observed in LSCO [26], Bi2201 [27] and in the antibonding sheet of Bi2212 [28]. In addition, we consider the  $d$ -wave electron pairing gap function  $\Delta_{\mathbf{k}} \equiv \Delta \cos(2\theta)$  with  $\Delta = 0.1t$ . The resulting  $dI/dV$  spectrum [see dash-dot line in Fig. 1(a)] depicts two sharp coherence peaks at  $V = \pm\Delta$  due to the SC quasiparticle energy dispersion  $E_{\mathbf{k}} = [\varepsilon_{\mathbf{k}}^2 + \Delta_{\mathbf{k}}^2]^{1/2}$  saddle-point at the SC gap en-

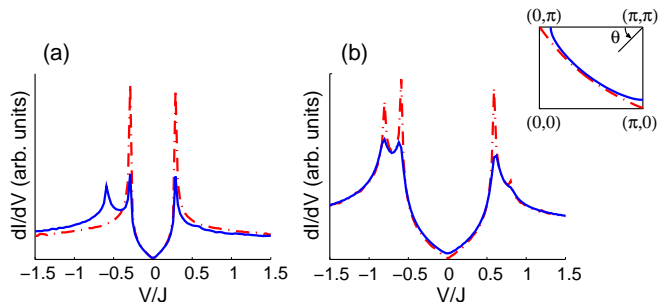


FIG. 1: BCS tunneling differential conductance for  $t' = -2t'' = -0.12t$  and: (a)  $\Delta = 0.1t$  with  $x = 0.20$  (dash-dot line) and  $x = 0.10$  (solid line); (b)  $\Delta = 0.2t$ ,  $x = 0.10$  with (solid line) and without (dash-dot line) Lorentzian broadening  $\Gamma = 0.01t$ . Bias is in units of  $J = t/3$ . Plots are obtained for a  $2000 \times 2000$  mesh of the Brillouin zone and energy resolution of  $0.0067t$ . Inset: Fermi surface of  $\varepsilon_{\mathbf{k}}$  with  $t' = -2t'' = -0.12t$  for  $x = 0.20$  (dash-dot line) and  $x = 0.10$  (solid line).

ergy. This behavior is consistent with experimental spectra around optimal doping [3, 4, 5, 12, 13, 14].

However, if the electron concentration is increased to  $1 - x = 0.90$  the normal state Fermi surface intersects the  $(0, \pi) - (\pi, \pi)$  line at a point, which we denote by  $\mathbf{k}_A$ , that moves away from  $(0, \pi)$  (inset of Fig. 1). In this case, the VH singularity in  $\varepsilon_{\mathbf{k}}$  at  $(0, \pi)$  and  $(\pi, 0)$  shows up as a separate peak in the BCS tunneling spectrum at  $V = -E_{VH} \equiv -[\varepsilon_{\mathbf{k}=(0,\pi)}^2 + \Delta^2]^{1/2}$  [Fig. 1(a)]. This additional peak appears behind the negative bias SC coherence peak unless  $\mathbf{k}_A \approx (0, \pi)$  or  $E_{VH} - \Delta$  is so small that spectral broadening smears the VH and the SC coherence peaks into a single feature. However, as shown in Fig. 1(b), the above double peak structure still survives if, as expected for real materials upon increasing electron concentration, the  $d$ -wave gap is doubled to  $\Delta = 0.2t$  and a broadening width  $\Gamma = 0.01t$  is included [29].

This behavior contrasts with the experimental observation that no such double peak structure occurs as the hole doping level is decreased [3, 5, 12, 13, 14] and implies that the actual dispersion along  $(0, \pi) - (\pi, \pi)$  in the cuprate materials is of the order of the SC gap energy scale, namely  $\sim 0.1t$ , which is an order of magnitude lower than  $t$ . Such a flat dispersion in the antinodal region is supported by ARPES data in Bi2201, Bi2212 and YBCO [20]. Since ARPES observations also constrain the much larger nodal dispersion energy scale, as well as the curvature of the Fermi surface, several fine-tuned phenomenological parameters are required to fit the observed normal state dispersions [Fig. 2(a) displays the dispersions obtained by Norman *et al.* from experimental fits involving up to five hopping terms [30, 31]]. As Ref. 32 points out, the ubiquitous discrepancy between the energy scale of the nodal dispersion and that of the extended flat region around  $(0, \pi)$  throughout the various cuprate families and doping levels suggests that

interactions strongly renormalize the electron dispersion. Below, we argue that such phenomenological dispersions are natural to doped Mott insulators.

*Renormalization of single electron properties* – To discuss how the single electron dispersion relation and the momentum space distribution of spectral weight are renormalized in doped Mott insulators we consider the  $tt't''J$  model, whose numerical calculations reproduce many spectral features of the cuprates [33, 34].

In the half-filled AF insulator, the electron dispersion is renormalized by the strong local AF correlations. In particular, NN hopping is heavily frustrated by the AF background and, for  $t' = t'' = 0$ , holes hop coherently within the same sublattice by virtue of spin fluctuations [35]. As a result, the width of the nodal dispersion is reduced by a factor of  $\sim 10$  from the bare value  $8t$  down to  $2.2J$  [33].  $t' \approx -2t''$  control the dispersion along  $(0, \pi) - (\pi, 0)$  and, since they describe intrasublattice hopping processes which are not frustrated by AF correlations, the dispersion width along this line is only renormalized by a factor  $\sim 2 - 3$  [33].

Away from half-filling, holes distort the AF spin background and change the surrounding spin configuration in order to coherently hop between NN sites and thus gain extra kinetic energy. Interestingly, exact diagonalization studies show that the resulting local spin correlations strongly renormalize  $t'$  and  $t''$  [36]. This effect, which is predicted in spin liquids [37], is consistent with the experimentally observed doping induced flatness of the dispersion in the antinodal region [20] since the dispersion along  $(0, \pi) - (\pi, 0)$  is controlled by  $t'$  and  $t''$ .

The “doped carrier” MF approach introduced in Refs. 18, 19 accounts for the above interplay between the exchange energy of localized spins and the kinetic energy of delocalized holes. Here, we present only a qualitative description of the MF theory and defer the readers to the above references for formal details. This theory describes doped Mott insulators in terms of two different fermions: (i) “dopons”, which have the same charge  $+e$  and spin-1/2 as holes, describe vacancies surrounded by an AF spin configuration; (ii) “spinons”, which have no electric charge, describe spin-1/2 excitations of the spin background. The MF Hamiltonian thus has four fermionic bands:  $\epsilon_{1,\mathbf{k}}^- = -\epsilon_{1,\mathbf{k}}^+$  and  $\epsilon_{2,\mathbf{k}}^- = -\epsilon_{2,\mathbf{k}}^+$  [Fig. 2(b)]. If dopons and spinons do not hybridize the high energy bands  $\epsilon_{2,\mathbf{k}}^\pm$  describe the dynamics of holes in an AF background and, at MF level, the spinon  $\epsilon_{1,\mathbf{k}}^\pm$  bands do not contribute to electron spectral properties. The process of hybridizing dopons and spinons, which describes the change in spin correlations due to hole hopping, couples spin and charge dynamics and transfers electron spectral weight from  $\epsilon_{2,\mathbf{k}}^\pm$  to the lower energy  $\epsilon_{1,\mathbf{k}}^\pm$  bands [Fig. 2(c)]. This spectral weight transfer is not uniform in momentum space and reflects the dispersion of the dopon band, which has lower energy at  $(\pi/2, \pi/2)$  than at  $(0, \pi)$ . As a result, the  $\epsilon_{1,\mathbf{k}}$  band has more spectral

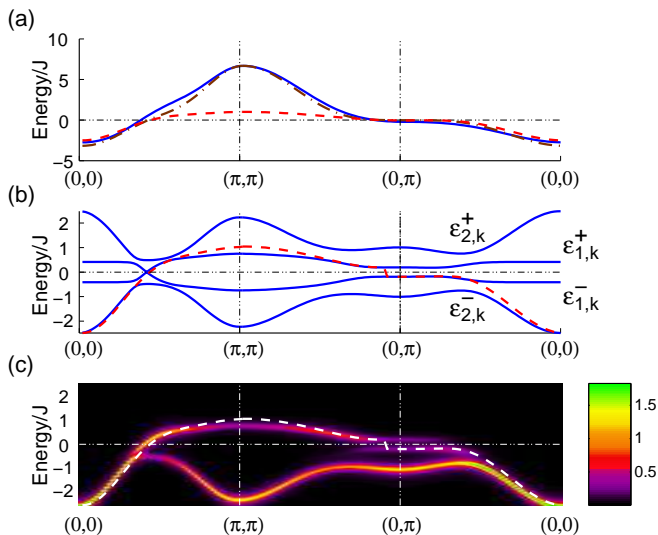


FIG. 2: Energy dispersions along  $(0,0) - (\pi, \pi) - (0, \pi) - (0,0)$ . (a) Normal state dispersions using parameters from Ref. [30] (solid line), Ref. 31 (dash-dot line) and  $\epsilon_{\mathbf{k}}^N$  defined in main text (dashed line). (b) MF dispersions  $\epsilon_{1,\mathbf{k}}^{\pm}$  and  $\epsilon_{2,\mathbf{k}}^{\pm}$  for  $x = 0.18$  and parameters used in Ref. 18. (c) MF spectral function with Lorentzian broadening  $\Gamma = J/5$  where  $J = 150\text{meV}$ . Dashed line in (b) and (c) plots  $[(\epsilon_{\mathbf{k}}^N)^2 + \Delta_{\mathbf{k}}^2]^{1/2} \times \text{sgn}(\epsilon_{\mathbf{k}}^N)$ .

weight near the nodal points than in the antinodal region [18], in agreement with the nodal-antinodal dichotomy in ARPES data [7, 8, 9]. In conformity with other approaches to the related Hubbard model [38], we conclude that this dichotomy results from short-range correlations, namely AF correlations [19, 36], in dSC.

The low energy dispersions  $\epsilon_{1,\mathbf{k}}^{\pm}$  derive from the spinon bands and, thus, from the spin exchange interaction. Therefore, they are controlled by a single energy scale, namely  $J$ , which leads to an almost flat dispersion near the antinodal points. We thus find that the spin background strongly renormalizes the electron dispersion in the antinodal region. To explicitly compare the MF dispersion with the experimental fits to ARPES data we introduce the underlying normal dispersion  $\epsilon_{\mathbf{k}}^N$  such that  $[(\epsilon_{\mathbf{k}}^N)^2 + \Delta_{\mathbf{k}}^2]^{1/2}$  equals: (i)  $\epsilon_{1,\mathbf{k}}^+$  at  $\mathbf{k}_A$ ,  $(0, \pi)$  and at the nodal point; (ii)  $\epsilon_{2,\mathbf{k}}^+$  at  $(0,0)$  [Figs. 2(b) and 2(c)]. In Fig. 2(a) we plot  $\epsilon_{\mathbf{k}}^N$  for  $x = 0.18$  against the normal dispersion fits from Refs. 30, 31 along major symmetry directions. Clearly, below the Fermi level  $\epsilon_{\mathbf{k}}^N$  captures the energy scale of the nodal dispersion and the flatness around antinodal points. ARPES does not probe the dispersion above the Fermi energy and both experimental fits use band calculation results to fix the energy at  $(\pi, \pi)$  [30], whence the mismatch between  $\epsilon_{\mathbf{k}}^N$ , obtained within the  $tt't''J$  model context, and these fits above the Fermi level. Such a mismatch is supported by exact diagonalization calculations of the  $tt't''J$  model which indicate that the dispersion above the Fermi level is less disper-

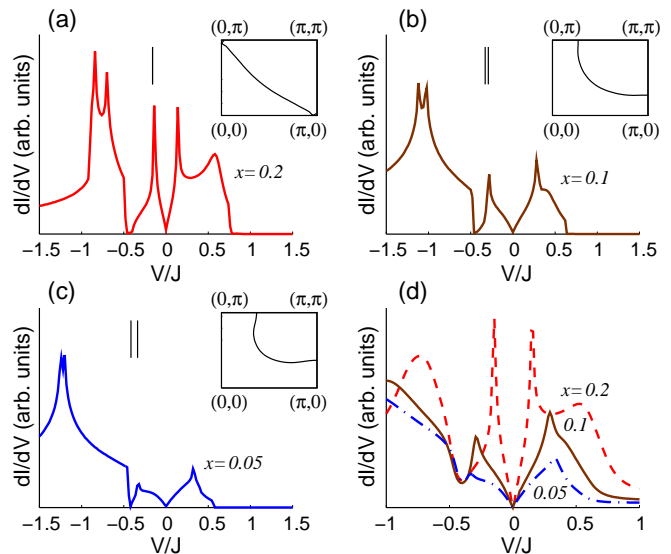


FIG. 3: MF tunneling differential conductance for (a)  $x = 0.20$ , (b)  $x = 0.10$  and (c)  $x = 0.05$ . (d) Same spectra with broadening given by  $\Sigma''(\omega) = -\omega^2/(5J)$ . Momentum space and energy resolution are the same as in Fig. 1. Insets of (a)-(c) plot minimal gap locus of  $\epsilon_{1,\mathbf{k}}^{\pm}$ . Vertical bars in (a)-(c) denote VH singularity and SC gap energies.

sive than expected from bare hopping parameters [34].

*Tunneling spectra of strongly correlated d-wave superconductors* – We now consider the tunneling conductance for the above MF theory of doped Mott insulators. We use the same parameters as in Ref. 18 to obtain the  $dI/dV$  curves at  $x = 0.20$ ,  $x = 0.10$  and  $x = 0.05$  [Figs. 3(a)-3(c)]. We point out that the MF theory produces a sharp electron spectral peak at the  $\epsilon_{2,\mathbf{k}}^{\pm}$  band. However, we expect this spectral peak to be significantly broadened if one goes beyond the MF approximation since  $\epsilon_{2,\mathbf{k}}^{\pm}$  are high energy bands which have many channels to decay. Hence, in order to better compare to experiments, in Fig. 3(d) we depict the above spectra with a frequency dependent broadening given by  $\Sigma''(\omega) = -\omega^2/(5J)$ .

Looking at Figs. 3(a)-3(c) we recognize the separate contribution to the tunneling DOS from bands  $\epsilon_{2,\mathbf{k}}^{\pm}$ ,  $\epsilon_{1,\mathbf{k}}^{\pm}$  and  $\epsilon_{1,\mathbf{k}}^+$ . The positive energy  $\epsilon_{2,\mathbf{k}}^+$  band does not appear since it has vanishing spectral weight [see Fig. 2(c)]. The presence of the negative energy bands  $\epsilon_{2,\mathbf{k}}^-$  and  $\epsilon_{1,\mathbf{k}}^-$  leads to a peak-dip-hump in the  $dI/dV$  curve as observed by experiments [5, 12]. This negative bias hump, which moves to higher energy as doping is lowered [5, 12], derives from the lower Hubbard band and renders the tunneling conductance plots highly asymmetric for large positive and negative bias. At smaller values of  $x$  the spectral weight in the  $\epsilon_{1,\mathbf{k}}^-$  and  $\epsilon_{1,\mathbf{k}}^+$  bands is transferred to the high-energy hump and, thus, the above bias sign asymmetry is enhanced upon underdoping as seen in STM data [3, 5, 6, 17]. In particular, the ratio of integrated spectral weight at positive bias over that at negative bias

is  $2x/(1-x)$ , in perfect agreement with sum rules applicable to the generalized- $tJ$  model [39]. The above behavior is a hallmark of models where strong local Coulomb repulsion between electrons makes it easier to add a hole to the sample than to add an electron.

Figs. 3(a)-3(c) depict the doping evolution of the minimum gap locus, which reproduces experiments [26], and denote the VH singularity and SC gap energies,  $E_{VH}$  and  $\Delta$  respectively, by the small vertical bars. Changing from  $x = 0.20$  to  $x = 0.10$  the wave vector  $\mathbf{k}_A$  distances from  $(0, \pi)$ , yet  $E_{VH} - \Delta$  remains extremely small since the dispersion is very flat in the antinodal region. Therefore, no extra peak develops next to the SC coherence peak, unlike the cases depicted in Fig. 1. The energy difference  $E_{VH} - \Delta$  increases for  $x = 0.05$ , yet, we observe a strong suppression of the SC coherence peak in the tunneling spectrum of Fig. 3(c) instead of a double peak structure. Below, we explain this behavior, which is in stark contrast with weak coupling BCS predictions.

The curves in Fig. 3 show how the SC coherence peak evolves with doping level. The  $x = 0.20$  spectrum displays well defined SC coherence peaks, in agreement with spectra of samples around optimal doping [3, 4, 5, 12, 13, 14]. In the underdoped  $x = 0.10$  spectrum the SC coherence peaks are pushed to higher energy due to the SC gap doping dependence and lose spectral weight, as seen in experiments [3, 5, 12, 13]. The spectrum for the SC state at  $x = 0.05$  hardly resolves the SC coherence peaks as found in deeply underdoped Bi2212 [3, 5] and NaCCOC [6, 17]. The gradual depletion of the SC coherence peak intensity as the half-filled state is approached follows from the correspondingly gradual depletion of spectral weight in the antinodal region which underlies the formation of the low energy spectral weight arcs observed both in ARPES experiments [7, 8, 9] and in theoretical approaches [18, 38]. In our calculation, this behavior explicitly results from the presence of short-range AF correlations in dSC.

As we emphasize in Fig. 3(d), the doping evolution of the  $dI/dV$  curves leads to qualitatively different line shapes around optimal doping and in the deeply underdoped regime. We refer to Fig. 2 of Ref. 5 to show that the above results reproduce experimental evidence for different types of spectra in SC cuprate materials. Since this STM spectral diversity occurs in samples which are inhomogeneous on the nano-scale [3, 4, 5, 17, 40, 41], it has been proposed that these non-trivial line shapes are intrinsically related to the presence of the underlying sample inhomogeneity [40]. The possible relevance of coexisting orders [5, 6] and phase separation scenarios [4, 17] has also been pointed out in the literature. However, here we show that the aforementioned unusual and diverse spectra can be reproduced in homogeneous SC systems solely due to the presence of strong correlations that follow from a proximate Mott insulating state. This theoretical assertion supports that electron dynam-

ics in these materials is, to a large extent, determined by properties which are local even when compared to the nano-sized sample inhomogeneities, in conformity with experimental results [41].

This work was supported by the Fundação Calouste Gulbenkian Grant No. 58119 (Portugal), by the NSF Grant No. DMR-01-23156, NSF-MRSEC Grant No. DMR-02-13282 and NFSC Grant No. 10228408 and by the DOE Grant No. DE-AC02-05CH11231.

- 
- [1] H. Matsui *et al.*, Phys. Rev. Lett. **90**, 217002 (2003).
  - [2] J.E. Hoffman *et al.*, Science **297**, 1148 (2002).
  - [3] S.H. Pan *et al.*, Nature **413**, 282 (2001).
  - [4] C. Howald *et al.*, Phys. Rev. B **64**, 100504(R) (2001).
  - [5] K. McElroy *et al.*, Phys. Rev. Lett. **94**, 197005 (2005).
  - [6] T. Hanaguri *et al.*, Nature **430**, 1001 (2004).
  - [7] X.J. Zhou *et al.*, Phys. Rev. Lett. **92**, 187001 (2004).
  - [8] F. Ronning *et al.*, Phys. Rev. B **67**, 165101 (2003).
  - [9] T. Yoshida *et al.*, Phys. Rev. Lett. **91**, 027001 (2003).
  - [10] W.-M. Que and G. Kirczenow, Phys. Rev. B **38**, 4601 (1988).
  - [11] A.J. Fedro and D.D. Koelling, Phys. Rev. B **47**, 14342 (1993).
  - [12] N. Miyakawa *et al.*, Phys. Rev. Lett. **83**, 1018 (1999).
  - [13] M. Oda *et al.*, Physica. C **281**, 135 (1997).
  - [14] M. Oda *et al.*, Supercond. Sci. Technol. **13**, R139 (2000).
  - [15] M. Kugler *et al.*, Phys. Rev. Lett. **86**, 4911 (2001).
  - [16] I. Maggio-Aprile *et al.*, Phys. Rev. Lett. **75**, 2754 (1995).
  - [17] Y. Kohsaka *et al.*, Phys. Rev. Lett. **93**, 097004 (2004).
  - [18] T.C. Ribeiro and X.-G. Wen, Phys. Rev. Lett. **95**, 057001 (2005).
  - [19] T.C. Ribeiro and X.-G. Wen, cond-mat/0601174 (2006).
  - [20] D.M. King *et al.*, Phys. Rev. Lett. **73**, 3298 (1994).
  - [21] D.J. BenDaniel and C.B. Duke, Phys. Rev. **160**, 679 (1967).
  - [22] J.Y.T. Wei *et al.*, Phys. Rev. B **57**, 3650 (1998).
  - [23] G.D. Mahan, *Many-Particle Physics* (Plenum, New York, 1990).
  - [24] Generically,  $t' \approx -2t''$  in the copper-oxide planes [25].
  - [25] E. Pavarini *et al.*, Phys. Rev. Lett. **87**, 047003 (2001).
  - [26] A. Ino *et al.*, Phys. Rev. B **65**, 094504 (2002).
  - [27] T. Takeuchi *et al.*, J. Electron Spectrosc. Relat. Phenom. **114-116**, 629 (2001).
  - [28] P. Bogdanov *et al.*, Phys. Rev. B **64**, 180505(R) (2001).
  - [29]  $\Gamma = 0.01t$  is consistent with experiments [4, 13].
  - [30] M.R. Norman *et al.*, Phys. Rev. B **52**, 615 (1995).
  - [31] M.R. Norman, Phys. Rev. B **61**, 14751 (2000).
  - [32] E. Dagotto *et al.*, Phys. Rev. Lett. **73**, 728 (1994).
  - [33] T. Tohyama and S. Maekawa, Supercond. Sci. Technol. **13**, R17 (2000).
  - [34] T. Tohyama, Phys. Rev. B **70**, 174517 (2004).
  - [35] C. Kane *et al.*, Phys. Rev. B **39**, 6880 (1989).
  - [36] T.C. Ribeiro, cond-mat/0605437.
  - [37] T.C. Ribeiro and X.-G. Wen, Phys. Rev. B **68**, 024501 (2003).
  - [38] D. Sénéchal and A.M.S. Tremblay, Phys. Rev. Lett. **92**, 126401 (2004).
  - [39] M. Randeria *et al.*, Phys. Rev. Lett. **95**, 137001 (2005).
  - [40] A.C. Fang *et al.*, Phys. Rev. Lett. **96**, 017007 (2006).

[41] K. McElroy *et al.*, *Science* **309**, 1048 (2005).